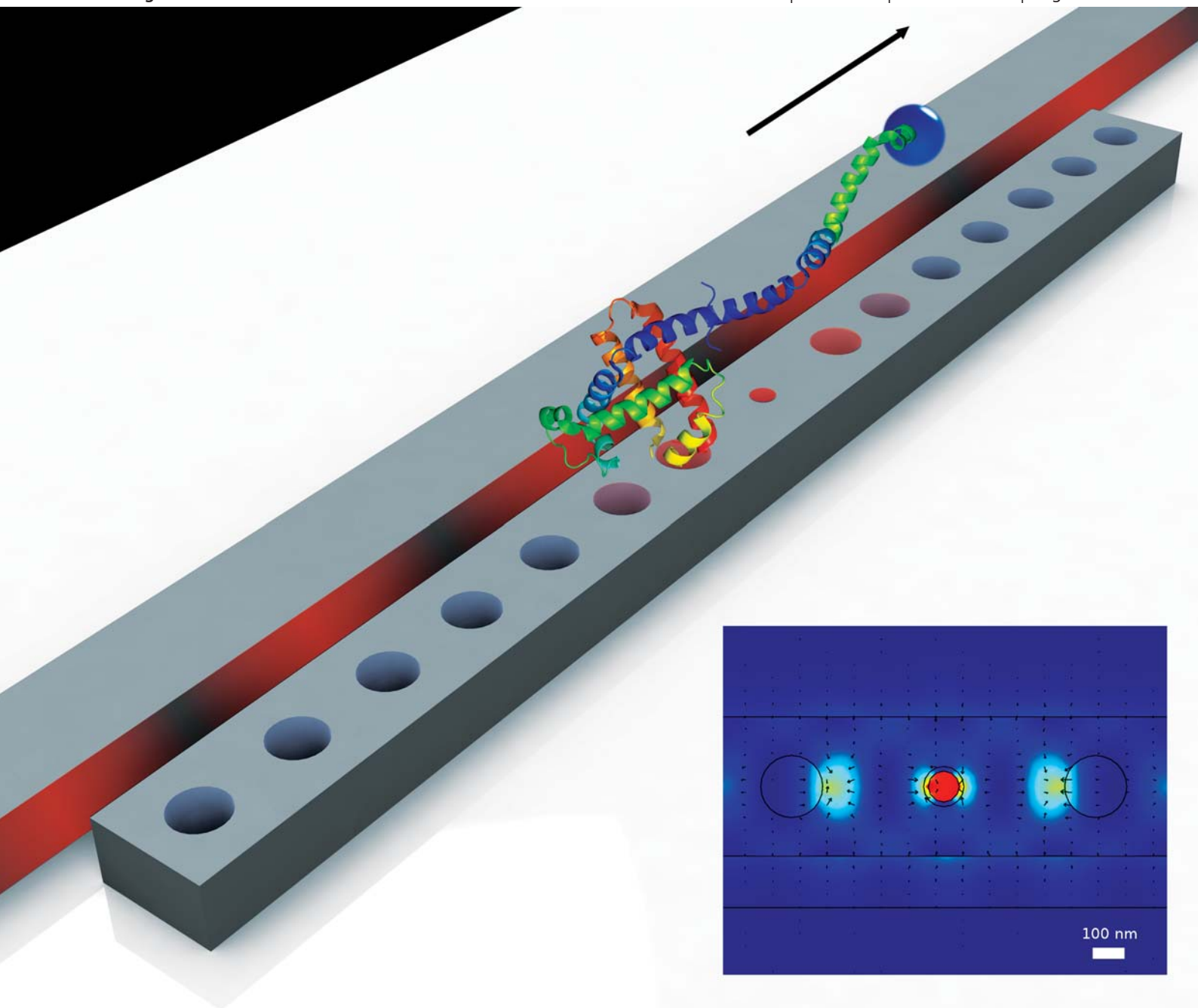


Lab on a Chip

Micro- & nano- fluidic research for chemistry, physics, biology, & bioengineering

www.rsc.org/loc

Volume 11 | Number 6 | 21 March 2011 | Pages 981–1176



ISSN 1473-0197

RSC Publishing

CRITICAL REVIEW
Erickson *et al.*
Nanomanipulation using near field photonics

Cite this: *Lab Chip*, 2011, **11**, 995

www.rsc.org/loc

Nanomanipulation using near field photonics

David Erickson,^{*a} Xavier Serey,^b Yih-Fan Chen^{ac} and Sudeep Mandal^a

Received 5th October 2010, Accepted 21st December 2010

DOI: 10.1039/c0lc00482k

In this article we review the use of near-field photonics for trapping, transport and handling of nanomaterials. While the advantages of traditional optical tweezing are well known at the microscale, direct application of these techniques to the handling of nanoscale materials has proven difficult due to unfavourable scaling of the fundamental physics. Recently a number of research groups have demonstrated how the evanescent fields surrounding photonic structures like photonic waveguides, optical resonators, and plasmonic nanoparticles can be used to greatly enhance optical forces. Here, we introduce some of the most common implementations of these techniques, focusing on those which have relevance to microfluidic or optofluidic applications. Since the field is still relatively nascent, we spend much of the article laying out the fundamental and practical advantages that near field optical manipulation offers over both traditional optical tweezing and other particle handling techniques. In addition we highlight three application areas where these techniques namely could be of interest to the lab-on-a-chip community, namely: single molecule analysis, nanoassembly, and optical chromatography.

1.0 Introduction

Optically based manipulation techniques are playing an increasingly important role in the operation of microfluidic and lab-on-chip devices. Such techniques can be split between direct methods, whereby light forces are used to directly manipulate particles in a flow (see a recent review by Grier¹ as well as several

other prominent examples²⁻⁵), and indirect methods where a light field can be used to trigger a change in the hydrodynamic or electrical conditions around a particle and thereby change its flow path (this includes electro-optic techniques such as that by Chiou *et al.*⁶ as well as other flow manipulation techniques⁷). In either of these cases the primary advantages of using optical methods are that they: are nonobtrusive, can be localized to the single particle level, do not require any on-chip infrastructure since the light manipulation is done off chip, can be changed on-the-fly, and are biologically safe at the proper wavelengths.

These traditional techniques however have significant limitations when applied to nanoscale manipulation. As we will expand

^aSibley School of Mechanical and Aerospace Engineering, Cornell University, Ithaca, NY, USA. E-mail: de54@cornell.edu

^bApplied and Engineering Physics, Cornell University, Ithaca, NY, USA

^cKavli Nanoscience Institute at Cornell University, Ithaca, NY, USA



David Erickson

Dr David Erickson is an Assistant Professor in the Sibley School of Mechanical and Aerospace Engineering at Cornell University where he directs the Integrated Micro- and Nanofluidic Systems Laboratory. Prior to joining the faculty in September 2005, Dr Erickson was a postdoctoral scholar at the California Institute of Technology (2004–2005) and he received his Ph.D. degree from the University of Toronto in 2004. Dr Erickson was born in Edmonton, Alberta, Canada in 1976.



Xavier Serey

Xavier Serey is a PhD student at Cornell University in the department of Applied and Engineering Physics. He is working under the supervision of Professor Erickson in the Integrated Micro- and Nanofluidics laboratory focusing his research on optofluidic photonic crystal resonators. He previously completed a Diplôme d'Ingénieur in Ecole Centrale Paris.

on in greater detail below, practical extension of optical tweezing below the range of about 100 nm for a dielectric target is extremely difficult since the trapping force is proportional to the 3rd power of radius. As such the direct manipulation of many biological and non-biological targets (*e.g.* small viruses, proteins, and small nanoparticles) which have sizes ranging from 50 nm to 5 nm are well beyond the range achievable with free space optics.

In an attempt to address this, over the last few years there has been a push to develop “lab-on-chip” compatible optical manipulation techniques based on the use of near field photonics. The conceptual difference between a near-field optical trap⁸ and a free space one is illustrated in Fig. 1. In this example a region of high refractive index (core) between two low refractive index regions (substrates) is used to confine light through total internal reflection. When such a system is downscaled to dimensions similar to the wavelength of light we refer to them as nanophotonic^{9,10} waveguides. Analogous to optical fibres, these waveguides can be used to guide light over very long distances on a chip with very little lengthwise dilution of the optical energy. Though the light is confined to propagate in a single direction, a non-propagating, exponentially decaying, component of this optical mode (referred to as the evanescent field) extends outside the waveguide. The degree of this extension depends on the refractive index contrast between the waveguide and the surrounding media,⁹ however is generally on the order of 100 nm or so. When a particle enters the evanescent field, this optical gradient partially polarizes it resulting in an extremely strong Lorenz force analogous to the trapping force in traditional optical tweezers (F_{grad} in Fig. 1(b)). The large contrast in the refractive index of the waveguide material and the surrounding fluid medium leads to an extremely sharp decay of the evanescent field enabling much smaller material can be handled using near field photonics than with other methods. When this particle is trapped within the evanescent field, a certain percentage of the photons which flow through the waveguide are either scattered (radiated in a random direction) or absorbed when they contact the particle. These scattering and absorption events result in an

additional momentum transfer to the particle in the direction of optical propagation, F_{scat} and F_{abs} , and thus a net forward velocity. As indicated by the force balance in Fig. 1(b) this forward momentum is impeded by fluid drag on the particle, which we indicate as F_{stokes} since it usually occurs within the low Reynolds number, Stokesian regime.

Fig. 1(c) shows an analogous near field trapping scheme where the evanescent field is generated by a surface plasmon. Surface plasmons are electromagnetic waves that exist at the interface between a metal and a dielectric. These plasmons are excited when the effective wavelength of an incoming light beam is matched to the resonant condition, which depends on a variety of geometric and physical properties of the system. At the resonance condition, these plasmons generate extremely large local enhancements of the field strength also enabling much smaller objects to be manipulated. As we will discuss in greater detail in section 3.3, there exists a number of possible implementation for this technique. In Fig. 1(c) we show a non-propagating version where a trapped particle is held in place through the F_{grad} force which acts to attract the particle to a surface bound metallic nanostructure.

The overall goal of this review is to introduce readers to the use of near field optical manipulation techniques in microfluidic devices and some of the new applications which may arise through their use. In the first section below we will cover in more detail the limitations of traditional optical manipulation techniques when applied to the nanoscale and alluded to how near field techniques offer advantages. In this section we also present a very basic review of the theory of nanoscale optofluidic transport at the level where it is just sufficient to describe the advantages/disadvantages. Following this we will review some of the recent implementations including those which exploit simple waveguides, optical resonators and plasmonic devices. Finally in the last section we discuss in detail 3 separate application areas for which near-field optical manipulation is of likely interest to the lab-on-a-chip community. These application areas are: single molecule analytics, nanoassembly, and optical chromatography.



Yih-Fan Chen

Yih-Fan Chen is a postdoctoral fellow at the Kavli Institute at Cornell. He received his M.S. in Applied Mechanics from National Taiwan University in 2004 and received his Ph.D. in Biomedical Engineering from the University of Michigan, Ann Arbor in 2010. During his doctoral studies, he conducted a series of single-molecule experiments using optical tweezers to study the mechanics in gene regulatory network. Currently he works on the design and fabrication of photonic

crystal resonators at Cornell for both directed nanoassembly and single-molecule analysis.



Sudeep Mandal

Sudeep Mandal was born in Mumbai, India, in 1983. During his doctoral research in Prof. David Erickson's laboratory, he focused on exploiting the unique optical properties of photonic crystals to enable various optofluidic functionalities. He received his PhD in Applied and Engineering Physics from Cornell University in February, 2010. He is currently a research scientist at GE Global Research. His research interests lie in the areas of optofluidics, optical sensors and X-ray optics.

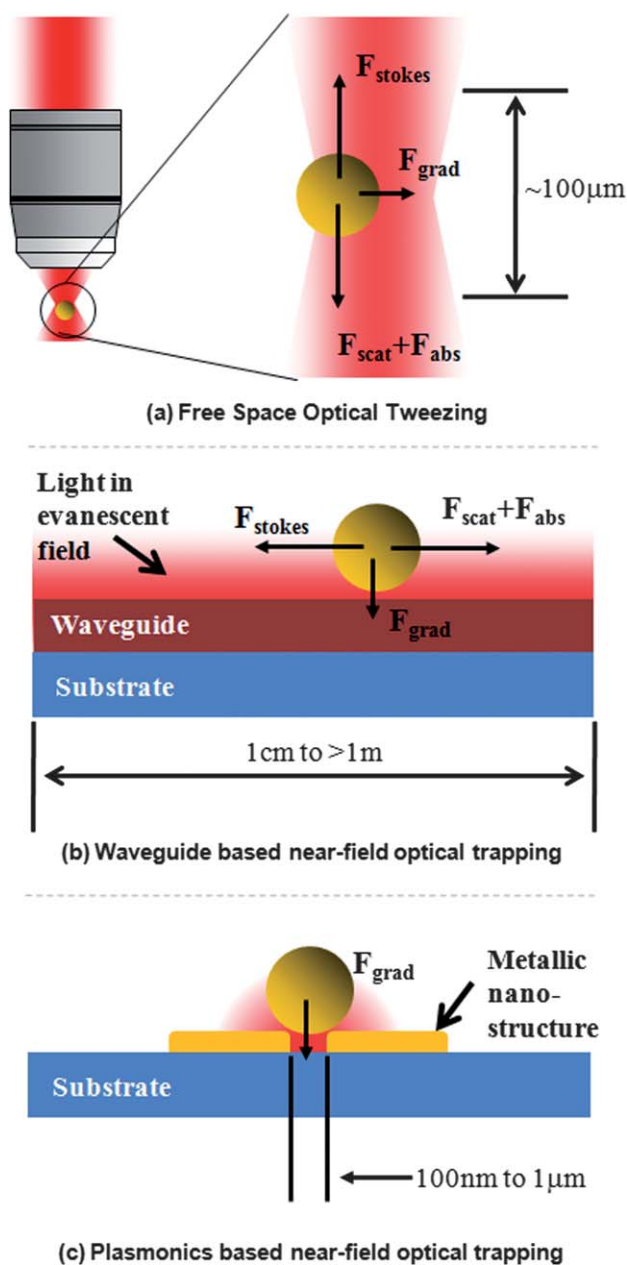


Fig. 1 Examples of traditional and near field optical tweezing/trapping techniques showing relevant forces. (a) Traditional single trap free-space optical tweezer. (b) Dielectric waveguide based near field optical trap. (c) Plasmonic near field optical trap.

2.0 Limitations of traditional optical manipulation systems when applied to the nanoscale

2.1 Brief review of optical trapping physics

Before proceeding we present a few general equations that can help describe the limitations of existing optical tweezing techniques when applied to manipulating nanoscale materials. As mentioned above, optical scattering and absorption forces exerted on a particle result from the momentum transfer of incident photons and act in the direction of optical propagation. For a spherical particle whose size is much smaller than the wavelength of light (a Rayleigh particle, see Svoboda and Block¹¹

and others^{12–14} for more details) these propulsive forces take the form,

$$F_{scat} = \frac{8\pi^3 I_o \alpha^2 \epsilon_m}{3c\lambda^4} \quad (1a)$$

$$F_{abs} = \frac{2\pi\epsilon_m I_o}{c\lambda} \text{Im}(\alpha) \quad (1b)$$

where $\alpha = 3V(\epsilon - \epsilon_m)/(\epsilon + 2\epsilon_m)$, V is the particle volume, c and λ are the speed and wavelength of light, ϵ and ϵ_m are the dielectric constants of the particle and material and I_o is the incident intensity. The dielectric constant is a function of wavelength and comprises of a real and an imaginary component, $\epsilon = \epsilon_1 + i\epsilon_2$. By convention, at optical frequencies these dielectric properties are expressed as a combination of the refractive index, n , and absorption coefficient, κ , as $\epsilon = (n + i\kappa)^2$. Conversion from a given refractive index or absorption coefficient to the complex dielectric constant can be done simply through the following two relations: $\epsilon_1 = n^2 - \kappa^2$ and $\epsilon_2 = 2n\kappa$. Note that in this paper when we use the term “dielectric” we are referring to materials in which have a relatively small absorption coefficient such that $\epsilon \approx \epsilon_1 \approx n^2$.

In the case where there exists a significant gradient in the intensity of the light field (such as in the evanescent field of a waveguide) the polarization induced force takes the form shown below.

$$F_{grad} = \frac{2\pi\nabla I_o \alpha}{c} \quad (2)$$

We note here that F_{grad} is positive when the gradient in intensity, ∇I_o , and α are of the same sign. In the case of a simple, non-absorbing, dielectric α is positive when the refractive index of the particle exceeds that of the surrounding medium. In this case particles will be attracted to the region of highest intensity (e.g. to the centre of a focused beam or to the surface of the waveguide). In the case where its refractive index is lower, it will be forced away from the region of highest intensity.

By equating the scattering and absorption forces with Stokes drag ($F_{drag} = 6\pi\eta a U_o$, where η is the viscosity and U_o is the particle velocity) we obtain,

$$U_o = \frac{\epsilon_m I_o}{6acn\eta} \left(\frac{8\pi^2 \alpha^2}{3\lambda^4} + \frac{2\text{Im}(\alpha)}{\lambda} \right) \quad (3)$$

which is descriptive of the speed at which a particle can be transported when it interacts with an electromagnetic field. To simplify the above we have ignored the contribution that a gradient force would have to the propulsion velocity.

2.1.1 More detailed theory on near field trapping. As mentioned, the above represents a very cursory introduction to some of the theory that governs near field optical trapping and transport and is mainly presented here to allow us to better explain some of the scaling advantages of near field optical transport and trapping. Much more detailed theoretical analyses of waveguide based propulsion have been presented for both Mie regime systems¹⁵ (for particles much larger than the wavelength) and the Rayleigh regime systems¹⁶ (where the electromagnetic field around the particle is relatively uniform). Almaas and Brevik¹⁷ and Ng *et al.*¹² also both deal specifically with the

behaviour of particles in evanescent fields. We have presented detailed numerical analysis of the conditions which lead to stable trapping on waveguides¹⁸ and comparisons between different optical resonator designs.¹⁹ Those interested in more detailed theory on near field optical forces are recommended to consult the excellent work by Novotny⁸ or some of the relevant references within Dholakia and Reece²⁰ (for example Quidant *et al.*²¹ and Brevik *et al.*²²).

2.2 Three fundamental limitations of applying free space trapping techniques to nanoscale manipulation

As mentioned above, traditional free space optical trapping techniques are difficult to apply directly to nanoscale manipulation. Here we point to three significant limitations that have particular relevance to the applications we will discuss later on and discuss how the use of near field techniques can help solve these limitations.

(1) Diffraction limit. It is well known²³ that the diffraction limit places a lower bound on size to which light can be focused. This minimum spot size diameter is given by $d_{min} = 1.2\lambda/NA$, where NA is the numerical aperture of the lens and λ is the wavelength. In an aqueous environment, light at 850 nm wavelength focused through a high numerical aperture lens has a d_{min} of approximately 550 nm. From eqn (1) and (2) above it is apparent that since light intensity is given by the input power divided by the illuminated area, this places a fundamental limitation on the trapping and propulsive forces that can be applied to a nanoparticle.

The most important consequence of this is that it essentially limits the useful range of optical tweezers to dielectric targets with sizes larger than about 100 nm.^{24,25} From eqn (2) it can be seen that extension to trapping of particles smaller than this limit is extremely difficult because the trapping force is proportional to the particle volume and therefore the 3rd power of radius. As such a 10 fold decrease in size to 10 nm requires a 1000 fold increase in some other parameter to maintain the same force. The propulsive case is worse still since the scattering force is proportional to the 6th power of radius (note though that since Stokesian drag is proportional to radius the velocity dependence is only proportional to 5th power of radius).

A number of authors have demonstrated optical manipulation of metallic nanoparticles^{11,26} and single dimensional nanowires.²⁷ In these cases the trap stability is dependent on exploiting the high absorption properties metallic structures (large κ) or the structures having at least one micrometre length scale (as in the nanowires). While manipulation of small highly absorbing materials is certainly important in a number of cases, most biomolecules and other biological systems have properties that are much closer to pure dielectrics and thus this advantage is not directly applicable to many of the applications of interest here.

As can be seen in eqn (2), the only other “knob” which can be turned to try and compensate for this fundamental decrease is the gradient force is the ∇I_o term (given that the material properties are fixed). This implies that the force can be increased by some combination of increasing the gradient of the light and/or its intensity. As we will see, the extremely high gradients in the evanescent field of nanophotonic devices coupled with the ability

of these devices to condense the electromagnetic energy to extremely small cross sectional areas greatly increases the magnitude of this term enabling us to apply greater forces to smaller particles.

(2) Light/species interaction length. Both the diffraction limit equation above and eqn (1a) and (1b) suggest that a simple way to increase the propulsive force would be to either reduce the wavelength of the laser or increase the effective numerical aperture (*e.g.* solid immersion lenses, SIL). Decreasing the wavelength to 488 nm would reduce the spot size by slightly less than half. The SIL technique has been developed in a number of different flavours^{28–30} with the general principal being that increasing the refractive index of the optical head gives one a nominal improvement in ultimate resolution ($1/n_i$). In either of these techniques the decrease in the spot size is necessarily offset by a proportional decrease in the depth of field. As such, although the spot size can be made smaller, the light/species interaction length becomes exceedingly small making it impossible to apply these optical forces on the nanoscale over distances more than a few micrometres.

Fortunately, some nanophotonic devices such as waveguides are explicitly designed to enable long distance transport of optical energy through the mechanism of total internal reflection. Optical fibres for example are designed to transmit light over kilometre scale distances with almost no dilution of the energy. As we will show below, the ability to apply optical forces over extended distances is a critical enabling technology in applications such as optical chromatography and nanoassembly.

(3) Thermal heating. All of the above equations show that the imparted force is directly proportional to intensity. Obviously then, the easiest way to increase these forces is to increase the optical power. The amount of power that can be applied however is limited by the thermal heating induced by absorption of the light in either the surrounding fluid or the target itself. This heating will eventually boil the liquid but will lead to direct damage to biological targets such as cells at much more moderate temperature increases. The amount of heating is strongly dependent on the conditions of the experiment (for example wavelengths in the 800 nm to 1100 nm range tend to absorb much less in water than others) but generally speaking an arrangement which has more favourable heat transfer characteristics will result in more rapid rejection of this heat and lower temperature increases for a given amount of input power.

While there have been a few recent studies examining the thermal conditions surrounding some near field trapping structures,^{31,32} to our knowledge there has not yet been a comprehensive study which directly compares the heat transfer advantages of near field trapping with free space techniques. Despite this we can make a few general comments. First, the majority of near field trapping experiments are done using a chip manufactured from a base wafer material of either fused silica or silicon. The thermal conductivity of fused silica is ~ 2.5 greater than that of water, quartz is between 10 and 17 times greater depending on the orientation with respect to the crystal plane, and silicon is close to 250 times greater. As a result, the thermal energy generated by absorption of the optical energy in the water surrounding a near field trap can be better rejected through the

underlying substrate than an equivalent amount could be rejected just through the water in a free space trap. The enhanced heat transfer effect is analogous to that for joule heating in electrokinetically based microfluidic systems³³ and was in fact one of the major cited motivations for development of chip based capillary electrophoresis systems.

The above argument assumes that the amount of electromagnetic energy that is converted to heat is comparable in both cases. Again, in the absence of a detailed study it is difficult to provide a direct comparison, but we can again make some general comments. Firstly, in the case of a dielectric near field trap (as opposed to a plasmonic one) a significant portion of the input power flows through the waveguide rather than the water. These waveguides tend to be made from materials that have relatively low absorption and thus for a given amount of input power there is likely to be less heat generated from such a system. Secondly, due to rapid thermal diffusion the size of the area which will experience significant temperature increase is likely to be much larger than the actual area which is illuminated. In such cases it is common to consider the heating element to be a “point source” (in the case of heating at a single point such as a free space trap or a small optical resonator/plasmonic nanoparticle) or a “line source” (in the case of heating along a line, which would be the more appropriate case for a waveguide). In these simplified cases the temperature profile is governed by a proportionality to the total input power. This is subtle but importantly different than the force equations above which are proportional to intensity. A major advantage of near field systems is that they allow one to increase the local intensity by condensing the light down to a smaller cross sectional area. *Via* the argument above then this allows one to increase the amount of force applied to a target, without increasing the amount of heat generated.

The above arguments are valid for low absorbing dielectric systems, but not necessarily for plasmonic trapping systems. Plasmons are generated using metal substrates which are high absorbers and therefore very efficient at converting electromagnetic energy to heat. Metal nanoparticles for example are proposed for use in a various photothermal therapy techniques whereby this heating is used as a method to locally kill cells. In the absence of a detailed comparative study, it is difficult to state how far this does towards reducing or fully eliminating the heat transfer advantages discussed above, but it is likely at least somewhat of a disadvantage.

3.0 Experimental implementations

In this section we review some of the recent experimental implementations of near field optical trapping focusing on those that have relevance to microfluidic systems. In each case we begin with a single or a few short case studies and then briefly review the state of the art. Although the mechanisms are similar, we split this section into three subsections with the first two covering trapping using planar dielectric nanophotonic devices (3.1 covers standard waveguides while in section 3.2 emphasizes the use of optical resonators) and plasmonic devices (section 3.3). We have tried to focus here on techniques which either demonstrate manipulation of nanoscopic material or show potential to do so

rather than provide a general review of all near field trapping implementations.

3.1 Planar waveguiding devices

Solid-core waveguide based devices are of particular interest because of the advantages they have when integrated with microfluidic systems. As explained above and shown in Fig. 1, such systems are designed so that this interaction generates optical scattering/absorption forces for propulsion and gradient (trapping) forces for confinement along the waveguide. The result is a sort of “optical train tracks” for nanoparticle transport and processing. Additionally, from a practical point of view, since optical waveguides can be run to the side of a microfluidic chip, they are relatively easy to couple light into and overlay microfluidic infrastructure without greatly disturbing either the optical or fluidic performance.

One of the earliest demonstrations of this technique was presented by Kawata and Sugiura³⁴ who demonstrated trapping and propulsion of 6.8 μm spheres in the evanescent field of light which has been totally internally reflected off a glass surface. Kawata and Tani³⁵ later extended this work to demonstrate the propulsion of large particles along a waveguide. The use of these techniques for true nanoscopic material manipulation was demonstrated in the 2000s in a series of papers by Ng *et al.*^{13,36} who showed the propulsion of colloidal gold nanoparticles (in the range of 17 nm to 23 nm in diameter) on traditional channel waveguides. Extensions of the technique to Y-branch waveguides for sorting of microparticles³⁷ and trapping and propulsion of biological cells³⁸ using silicon nitride waveguides were done a few years later.

Although these and other works^{39,40} have shown propulsion of dielectric particles along waveguides within static fluid cells, practical implementation of these techniques in a microfluidic system requires one to be able to directly capture particles initially carried within a pressure driven flow in a microchannel and transport them stably (*i.e.* without being “blown off”) both perpendicular to and opposite to the imposed flow. We (along with our collaborators in the Michal Lipson lab at Cornell) demonstrated this level of integration in 2007 using a platform based on planar SU-8 waveguides integrated with PDMS microfluidic channels.⁴¹ Note that details on the opto-hydrodynamic conditions which lead to this stable trapping can be found in Yang and Erickson.¹⁸

As shown in Fig. 2, the platform used in these experiments is comprised of SU-8 epoxy-based photonic structures, combined with poly(dimethylsiloxane) (PDMS) microfluidics on a fused silica substrate. The particles used in this experiment were polystyrene spheres with refractive index $n = 1.574$ in a 100 mM phosphate buffer solution (PBS) with a regulated pH of 7.0. The light source used for testing was a fibre coupled laser diode module with a wavelength of $\lambda = 975$ nm. In the experiment the dielectric particles are convected along with the pressure driven flow in the main microfluidic channel. When a particle comes in contact with the optically excited waveguide it may be captured in the evanescent field and begin moving in the direction of optical propagation. Fig. 2(d–e) shows time step images of the particle becoming trapped on the waveguide and propelled in the direction opposite the initial flow. More details are provided in

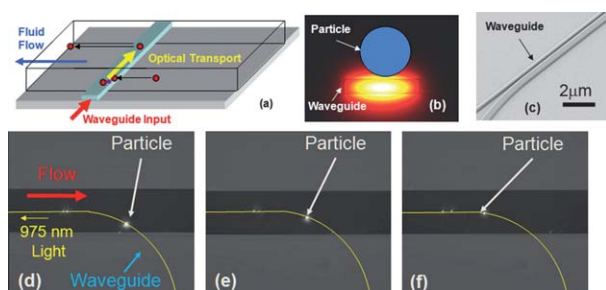


Fig. 2 Optical trapping and transport in the evanescent field of an optical waveguide. (a–b) A particle flowing in a microchannel becomes captured in the evanescent field of the excited waveguide. (c) SEM of two waveguides. (d–f) Time step images showing transport of 3 μm polystyrene particles on a waveguide.

the Schmidt *et al.*⁴¹ paper, broadly speaking however this trapping exhibited a dependence on pressure driven flow speed and the waveguide optical power. In particular, a greater portion of the particles are captured at lower flow speeds and higher optical powers. The propulsion speed along the waveguide exhibited a linear dependence on the excitation optical power reaching speeds on the order of 10s of μm 's per second. Though the limits of size trapping stability were not pushed, dielectric particles on the order of 500 nm in diameter could be manipulated with this technique.

3.1.1 Advanced waveguiding devices. Increasing the trapping force to be able to handle materials smaller than those described above necessarily requires that ∇I_o be increased as can be seen from eqn (2). Beyond simply increasing the power of the excitation laser, this can be done by either: (1) condensing the optical power down to a smaller cross sectional area, (2) increasing the “sharpness” of the gradient, or (3) through local amplification of the field.

One method by which the first two of these methods can be enhanced is through the use of “liquid core” waveguiding structures. The commonality between all liquid core structures used in optical trapping is that rather than interacting solely with the evanescent field, trapped targets are able to access the direct optical mode which is normally inaccessible inside the solid core of a standard ridge waveguide (as shown in Fig. 2b). An early attempt at this was the use of liquid core photonic crystal fibers⁴² in which particles were transported for very long distances (~ 10 cm) along the axis of the fibre. More recently work has been done using ARROW type waveguides (see papers by Schmidt and Hawkins^{43,44} for a review of the state of the art up to 2008). While direct optical trapping in these systems is still limited by the size of the optical mode (on the order of a few micrometres), such devices can be used for electro-optic trapping of small materials⁴⁵ where the guiding properties of the waveguide can be used to facilitate observation and electrokinetic effects can be used for target stabilization along the waveguide axis.

One type of waveguide that is perhaps more appropriate for direct manipulation of nanomaterials are silicon “slot waveguides”.^{46,47} These devices consist of a standard single mode silicon waveguide with a sub-wavelength slot (usually between 50 nm and 120 nm wide) cut through the middle as shown in Fig. 3. As has been demonstrated⁴⁸ and is shown in Fig. 3(b) this

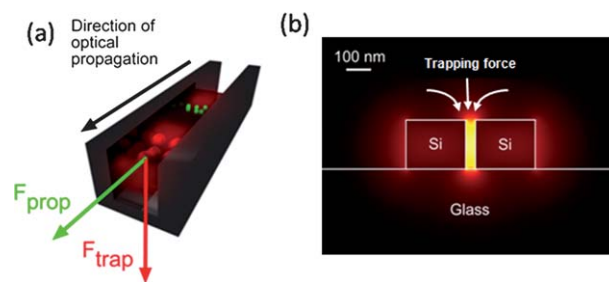


Fig. 3 Silicon “slot waveguide” nanoscale trapping structure. (a) Schematic of waveguide. (b) Mode profile showing trapping location. Reprinted with permission from Yang *et al.*⁴⁶

slot serves to concentrate the optical energy in the liquid core region of the waveguide. In 2009 our group and our collaborators in the Michal Lipson group at Cornell, used these slot waveguides to both trap and transport 75 nm dielectric particles.⁴⁶ As shown in Fig. 4 we have also been able to both capture from solution and stably trap individual strands of YOYO-1 tagged 48 kb long λ -DNA molecules. Readers are also referred to Yang and Erickson for more details on the analysis and trapping stability of these devices.⁴⁷ Although capable of handling much smaller objects, a disadvantage of using silicon devices is that they are only transparent in the 1550 nm wavelength range where the absorption in water is relatively high. The enhanced heat transfer in these devices (see section 2.2) serves to negate this effect to some degree, but it is certainly sub-optimal to have to work at this wavelength range.

3.2 Optical resonators

Referring back to the statement at the beginning of section 3.1.1, pushing the limits of optical force based manipulation can only be obtained by increasing the intensity of the field and “sharpness” of the gradient, or through local amplification/concentration of the electric field (*i.e.* increasing the local intensity above that which would be expected for a simple “flow through” waveguide). The slot waveguide technique described above demonstrates the first two of these methods. In these final two

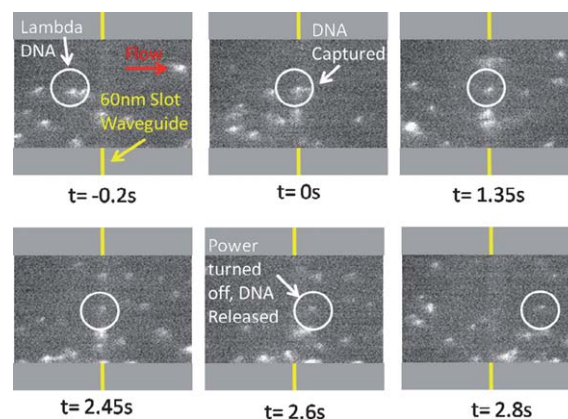


Fig. 4 Capture and trapping of λ -DNA. Images show individual YOYO tagged 48 kb λ -DNA trapped and released over a 60 nm slot waveguide. Reprinted with permission from Yang *et al.*⁴⁶

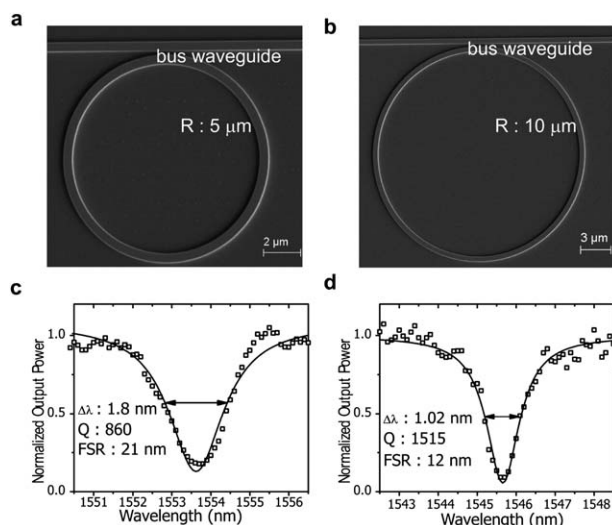


Fig. 5 SEM images and transmission spectra of microring resonators. (a,b) SEM image of micro-ring with radii of (a) 5 μm and (b) 10 μm . (c,d) Transmission spectra of rings with radii of (c) 5 and (d) 10 μm , respectively. Black squares are measured output powers. Lines are the Lorentzian fits to the measured data. The quality factor (Q) of the 10 μm micro-ring is 1515, which is larger than that of the 5 μm micro-ring ($Q = 860$) due to a smaller bending loss. Free spectral range (FSR) and the full width of the half-maximum of the resonance peak ($\Delta\lambda$) are also shown in (c,d). Reprinted with permission from Lin *et al.*⁴⁹ Copyright 2010 American Chemical Society.

subsections we cover methods for addressing the third, beginning with the use of optical resonance.

The easiest way to explain the use of optical resonance as it applies to optical trapping is through the ring resonator example shown in Fig. 5 presented originally by Lin *et al.*⁴⁹ In this case light at a given wavelength is sent down the bus waveguide. When the light encounters the ring beside the waveguide, a portion of the light becomes evanescently coupled into it and begins to circulate.⁵⁰ Resonance occurs when the incoming light is in phase and therefore constructively interferes with the light already circulating in the resonator. This occurs when the distance around the ring is an integer multiple of the effective wavelength of the light in the ring. The end result is that when it is excited at resonance there exists a stronger optical intensity confined in the resonant structure relative to the bus waveguide.⁵¹ This strong coupling correlates with a sharp drop in the bus waveguide power output, which can be seen in Fig. 5(c) and (d). Optical resonators are characterized by the Q -factor which is the ratio of the energy stored in the resonator divided by the energy dissipated per cycle (multiplied by 2π). The Q -factor of a resonator can be estimated by dividing the resonant frequency, f_r , by the full width half maximum, Δf_{fwhm} , of the peak or dip in the transmission spectrum ($Q \approx f_r / \Delta f_{fwhm}$). Though there are a number of practical difficulties with optical trapping on very high Q resonators, in principal when two similar device geometries are compared the greater the Q factor the greater the electric field intensity in the evanescent field of the resonator which leads to a greater trapping force.

The use of ring resonator or similar devices for optical trapping has been demonstrated by a number of authors. In the paper discussed above Lin *et al.*⁴⁹ demonstrated the trapping of 1.1 μm

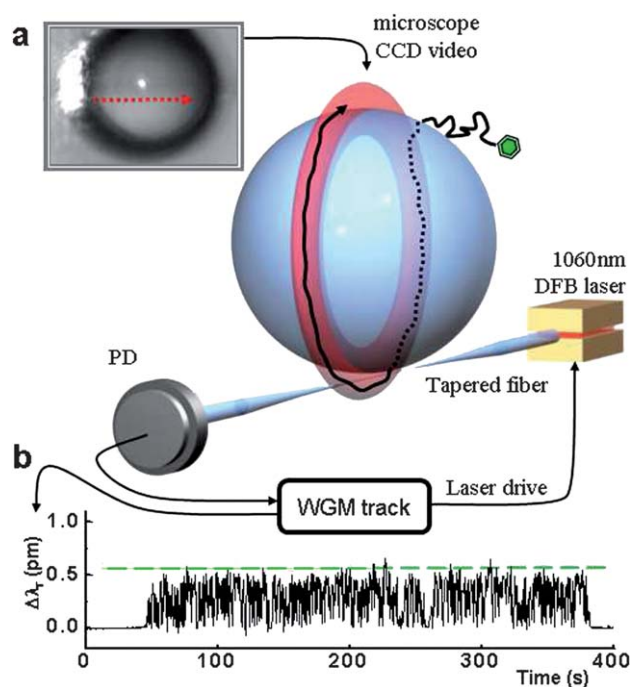


Fig. 6 WGM-carousel-trap. (a) WGM excited in a microsphere (radius $R = 53 \mu\text{m}$) with $Q = 1.2 \times 10^6$ by a 1060 nm tunable laser using fiber-evanescent-coupling. The resonance wavelength is tracked from a dip in the transmitted light (PD). An elastic scattering image shows a polystyrene particle (radius $a = 375 \text{ nm}$) trapped and circumnavigating at $2.6 \mu\text{m s}^{-1}$ using a drive power of $32 \mu\text{W}$. (b) A particle is sensed through resonance wavelength fluctuations $\Delta\lambda_r$ that identify its size/mass. These fluctuations are recorded from before the particle enters the Carousel-trap until after it escapes $\approx 6 \text{ min}$ later. Copyright Optical Society of America. Reprinted with permission from Arnold *et al.*⁵³

diameter particles on silicon ring structures. The transport speeds of the particles as they circulated around the rings as a function of wavelength was characterized with the peak velocities shown to be slightly redshifted from the resonance condition. The positional stability in the circular orbit was also characterized. Yang and Erickson⁵² demonstrated the trapping of similarly sized particles on SU-8 rings. In one of the first studies to exploit this phenomena, Arnold *et al.*⁵³ demonstrated the trapping and transport of polystyrene nanoparticles as small as 280-nm in diameter in a circular orbit around a whispering gallery mode (WGM) resonator possessing a Q -factors as high as 10^6 . The system geometry used in this experiment is shown in Fig. 6 below. They reported polar velocities on the order of $2.6 \mu\text{m s}^{-1}$ using very low excitation powers ($32 \mu\text{W}$).

While ring resonators and similar devices have significant advantages in terms of ease of fabrication and potentially very high Q -factors, a limitation they have is in “non-localization” of the field. What we mean by this is that if a particle is trapped on the ring, it is propelled around it and there is no preferential location where one would expect to find the particle along the orbit. We have attempted to address this shortfall through the use of planar photonic resonators similar to that shown in Fig. 7. Our current design, consists of a silicon (Si) waveguide with a 1D photonic crystal⁵⁴ micro-cavity⁵⁵ that lies adjacent to the waveguide. For the case shown here the side resonator consists of

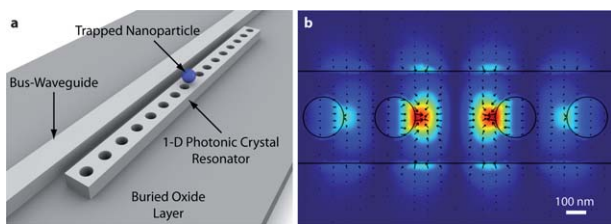


Fig. 7 Photonic crystal resonator for enhanced optical trapping. (a) 3D schematic of the one-dimensional photonic crystal resonator optical trapping architecture (b) 3D FEM simulation illustrating the strong field confinement and amplification within the one-dimensional resonator cavity. The black arrows indicate the direction and magnitude of the local optical field gradients. Reprinted with permission from Mandal *et al.*⁵⁶

a central defect cavity with 8 holes on either side which form the 1-D photonic crystal. Analogous to the ring resonators, when light at the resonant wavelength is coupled into the bus-waveguide, a stationary interference pattern is formed within the photonic crystal resonator resulting in a tight confinement and amplification of the optical field in an extremely small volume as illustrated in Fig. 7b. To demonstrate the technique, we conducted an experiment similar to those shown above for the slot waveguide. As can be seen in Fig. 8 when the resonator is optically excited the 60 nm polystyrene spheres flowing by are captured in the cavity and held there until either the wavelength is changed (taking the device off resonance) or the optical power is reduced.

3.3 Plasmonics

The behaviour of light about metallic nanostructures has been long investigated starting with Mie's (1908) and Ritchie's (1957) seminal works.^{57,58} It is now well understood how coherent oscillation of valence electrons in metals (surface plasmons or plasmon polaritons) lead to field enhancement and absorption.⁵⁹ These excitations come in two types, surface plasmon resonance for flat surfaces, and localized plasmon resonance for nanometre scale metal structures. Thanks to recent advances in nanofabrication,⁶⁰ plasmonics found applications in diverse fields such as chemistry,⁶¹ photonics,^{59,62} optical manipulation,⁶³ and are used in commercial products such as pregnancy tests. In near field manipulation, the diversity of plasmonic effects appears as a driving factor of plasmonic trapping.

Both surface plasmon resonance (SPR) and localized surface plasmon resonance (LSPR) have been used to enhance trapping forces without generating much unwanted heat. The trapping forces of conventional optical tweezers can be enhanced about 40 times, at a given incident intensity, by SPR according to the experiment done by Volpe *et al.* using photonic force microscopy (PFM).⁶⁴ To utilize the surface plasmon-enhanced optical forces to trap particles at specific locations, either a patterned incident light⁶⁵ or a patterned metal surface is required to provide an additional in-plane field confinement.^{66–68} Instead of using a highly focused laser beam, which is normally used in conventional optical tweezers setup, surface plasmon-based optical traps can provide enough trapping with non-focused illumination, and the required light intensity is significantly lower than that of conventional ones. By exciting surface plasmons on gold



Fig. 8 Trapping of nanoparticles on photonic crystal resonator. The waveguide is excited at the resonant wavelength while 60-nm particles flow through a microfluidic channel running over the resonator and the waveguide. The yellow circle tracks the 60-nm particle which is trapped (indicated by orange circles) on the resonator. Turning the laser power off releases the particle from the trap. Reprinted with permission from Mandal *et al.*⁵⁶ Copyright 2010 American Chemical Society.

discs on the top of a glass substrate, parallel and size-selective trapping of polystyrene particles has been demonstrated.^{66,67} However, because of the illumination asymmetry in the experimental geometry in the aforementioned papers by Righni *et al.*,^{66,67} the enhanced local field is also asymmetric, and a stable trapping of Rayleigh particles is prevented. To demonstrate the potential of plasmonic trapping for lab-on-a-chip applications, similar plasmonic nanostructures have been integrated with microfluidic channels to trap yeast cells.⁶⁹ In addition to using SPR to enhance 2D confinement, LSPR in gold and silver particles, which exhibit strong plasmon resonance, have also been used to increase the gradient forces of 3D optical traps. Grigorenko *et al.*⁶⁸ demonstrated that, for example, by illuminating pairs of gold nanodots with a focused laser beam, the localized plasmon resonance between two closely spaced nanodots can generate a strong optical trap that can improve the positioning of particles by almost an order of magnitude as compared to conventional optical tweezers. In another experiment, plasmonic dipole antennas were used as a field enhancement mechanism to trap 10 nm gold particles.⁷⁰ In these 3D traps, particularly high performances are achieved due to the fact that the particle experiences the full field strength rather than an evanescent field. Since the resonance frequency of the localized surface plasmon is very sensitive to changes in the dielectric constant of the gap, the antennas can also work as sensors for detecting trapping events.

Other plasmon-based phenomena have been investigated for trapping. For example, surface plasmons contribute to the trapping mechanism in the particularly successful self-induced back-action trap published by Juan *et al.*⁷¹ in 2009. The authors demonstrate trapping figures of merit an order of magnitude higher than the state of the art. They make use of the induced resonance when a particle enters a small aperture in a metal film being illuminated at a wavelength just below its cutoff frequency. Another example is the propulsion of gold nanoparticles above a gold stripe, where the propelling forces arise from the propagation of a SPR and from the near-field coupling between two gold structures rather than the evanescent field from a dielectric surface.⁷² In a later paper, Wang *et al.*⁷³ experimentally use the superposition of two counterpropagating SPRs to achieve tunable localization of a dielectric particle on the surface of a gold stripe, as shown in Fig. 9. When illuminating the gold stripe at two different positions, the radiation pressures resulting from the two counterpropagating SPRs cancel out at a certain position. By changing the relative intensities of the illuminating sources, the position where the two forces balance each other, which is essentially the trap center, can be tuned along the gold

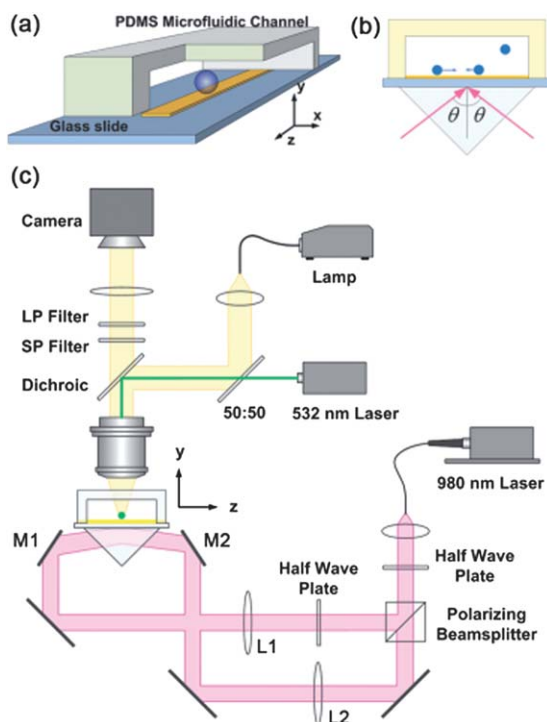


Fig. 9 (a) Schematic of plasmonic trapping device, consisting of a gold stripe in a microfluidic channel formed on a microscope glass slide. (b) Schematic of prism coupling of counterpropagating SPPs on gold stripes. (c) Schematic of optical setup: LP filter, long pass filter; SP filter, short pass filter. Reprinted with permission from Wang *et al.*⁷³ Copyright 2010 American Chemical Society.

stripe. This design is potentially very useful because it provides more flexibility on the manipulation of trapped objects.

4.0 Applications

In this section, we will expand on some of the potential new applications that nanophotonic based optical manipulation could enable. Although numerous applications can be envisioned, we focus here on the three areas that we feel are most promising. In each of these cases we begin with a small amount of background on the topic, describe the potential advantages that nanophotonic manipulation could offer and then, cover any relevant preliminary work that has been done in the area.

4.1 Biological trapping of single molecules

As reviewed by Borgia *et al.*,⁷⁴ Moerner,⁷⁵ Schuler and Eaton⁷⁶ and Uversky *et al.*⁷⁷ there are a number of significant challenges in single molecule analysis. One prohibitive one is that the diffusion of small molecules in solution is extremely fast and thus it is difficult to observe the target in free solution for longer than the time required for it to move across a microscope field of view. Depending on the size of the molecule and the numerical aperture of the lens, this can be less than a millisecond. To prolong this observation time numerous physical immobilization methods have been developed including: substrate tethering,⁷⁸ electrostatic pinning,^{79,80} spin-casting in biopolymers,⁸¹ nanovesicle confinement^{82,83} or confinement within nanochannels.^{84–86}

As is discussed in detail by Moerner,⁸⁷ however the act of using these physical confinement methods perturbs the natural, free solution, behaviour of the molecule. For example, in protein folding studies surface tethering directly disrupts the molecular structure, and physical confinement in structures with charged walls will induce electrostatic interactions. Nanovesicle confinement and some spin casting techniques which enclose the target molecules inside a confined but comparatively large volume minimize this but complicate other aspects of single molecule analysis. Since the confining volumes are by definition sealed off with these techniques, they have limited applicability to studies related to understanding how interactions differ in response to changes in external environmental conditions. As a result of this there has been significant interest in developing “free solution” immobilization techniques which can enable long term study of single molecules.

The ideal tool to facilitate these single or few molecule interaction studies, would be one that could: (1) capture and suspend small molecules in free solution for an indefinite period of time, (2) allow rapid modulation of the external environmental conditions, and (3) effectively “concentrate” the set of molecules of interest to a point where intermolecular interactions can be studied. The latter of these is critically important since few-molecule experiments are normally performed at extremely low concentrations (between 10^{-9} M and 10^{-12} M) to separate molecules spatially for optical detection. As such waiting for two molecules to come close enough to interact can take an incredibly long time. The development of a system which meets these three criteria could find application not only in the study of protein-protein interactions but also in protein folding/aggregation studies (to help elucidate binding mechanisms in the development of pharmaceuticals) and enable the more rapid analysis of individual nucleic acids for direct sequencing and haplotyping.^{88–90}

4.1.1 Opportunities for nanophotonic trapping in single molecule analysis. In this context, nanophotonic devices have several important advantages over the state of the art, which we list and discuss here.

(1) *Extremely high trapping stability.* From eqn (2) the trapping force is proportional to the gradient in the intensity. The extremely high decay rate of the optical energy outside these devices leads to the very high trapping force. To enable long timescale trapping of molecule however, what is required is not just a large absolute force but rather the work required for the particle to escape from the trap should be much greater than the random thermal energy k_bT . One way this can be quantified is through the following relation,

$$S = \frac{\int_{r_o}^{\infty} F_{grad} dr}{k_b T} \quad (4)$$

Where r is spatial coordinate that describes the path of least resistance for a trapped particle to move from its equilibrium position, r_o , to some distance far away. S is a value we have referred to as the stability factor¹⁸ for simplicity, but should be understood to simply be the ratio above. In eqn (4) we use include just the F_{grad} component of the force since this is likely to

Table 1 Trapping Stability for a 100 nm diameter polystyrene bead

Trapping Method	Stability factor at 300 K (W^{-1})	Decay length (nm)
Microcavity design (MD)	9000	60
Mode gap design (MG)	26000	55
Microcavity plus hole (MH)	44000	50
Slot waveguides, 65 nm diameter particle	875	50–100

be the most significant, but in principal all relevant optical forces should be accounted for.

An example of the use of the practical application of the stability factor is presented in Serey *et al.*¹⁹ who used it to compare a number of resonator designs to determine which would exhibit the most stable trapping for small dielectric objects. Table 1 shows an example of the results for the 3 1D silicon optical resonator designs shown in Fig. 10, normalized by 1 watt of input optical power compared with the result for a 65 nm particle trapped in a slot waveguide. These cases are all for relatively large particles which would rest on top of the resonator and not be trapped within the “hole” for the MG and MH designs. The decay length is the 1/e decay length for the evanescent field in each of these cases. The study went on to show that for a 40 nm polystyrene particle the “microcavity plus hole” design would have a stability on the order of 70 000 W^{-1} (for a particle which enters the hole, as opposed to resting on top of it). While at this point it is difficult to expand this theory to predict what the ultimate size limit would be, the extremely high stability numbers above do suggest that it is well below what has already been achieved and likely below 10 nm.

Physically, the stability factor is representative of the magnitude of the potential barrier which a particle must surmount in order to be released from the trap. It can therefore, in principal, be used as a predictive measure as to what the average amount of time a particle is likely to be trapped for (see Yang *et al.*⁴⁶ for an example). Due to the lack of detailed theory at the very small scale however, the stability factor as presented above is likely best used as a comparative value rather than a quantitative measure of trapping time.

(2) *Ability to dynamically change the local environment.* Unlike some of the other single molecule confinement techniques, nanophotonic traps provide direct access to the solution which can be modulated microfluidically. Doing this would be conceptually a relatively simple extension of the trapping experiments demonstrated above. Other fluid dynamically based trapping techniques also have this capability. For example Cohen and Moerner⁹¹ developed an electrokinetically based trapping system which, with the aid of an extensive optical-electrical feedback mechanism, was able to trap single semiconductor quantum dots (diameter ~ 10 nm) for over 10 s in a glycerol–water solution. This system relies on an active feedback mechanism in which manipulation of a series of high strength electrical fields are used to “beat” Brownian motion and the use of glycerol to increase the solution viscosity. This technique has recently been improved upon⁹² to the point where single proteins can be trapped in buffers, however the technique

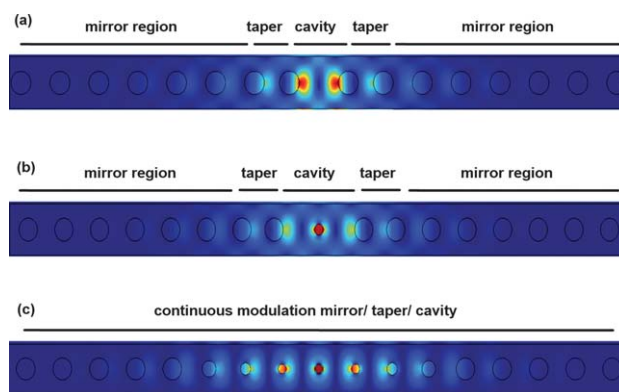


Fig. 10 Optical resonator designs compared in Table 1. Reproduced from Serey *et al.*¹⁹ Copyright Institute of Physics.

remains complicated and requires extensive feedback control to maintain stability.

(3) *Ability to reject heat more efficiently.* As mentioned in section 2.2 above, since the trapping occurs near a surface the effective thermal conductivity is higher and the heat can be rejected more efficiently.

4.2 Directed nanoassembly

Self-assembly^{93–95} is the easiest possible manufacturing technique. Put simply, the idea is one begins with a set of assembly elements (for example nanoparticles, small molecules or electronic components) with some inter-element attraction affinity relationship. When the assembly elements are mixed together and then allowed to settle to their equilibrium state, this affinity relationship uniquely determines both how the elements will assemble and, in principle, what the final structure will be. By extension then, in an engineered system a manufacturer should be able to design the affinity relationship between the assembly components and produce a desired structure. This approach forms the basis of most self assembly techniques and has successfully demonstrated using a large number of different affinity relationships some of which include: nucleic acid recognition,^{96–101} geometric/surface tension based interactions^{102–107} and a variety of charge or surface energy based techniques^{108–113} (see reviews by Grzybowski *et al.*⁹³ or Glotzer *et al.*⁹⁵ for more details). In practice, the types of structures that can be best created with the above “hands-off” technique tend to be either: very regular (such as with the photonic crystals assembled from colloidal particles^{114–116}), very irregular (as with DNA polymers¹¹⁷) or involve the assembly of only a small number of different components (as with fluidically driven assembly of small circuits and LEDs^{104,118}).

“Directed” self-assembly attempts to expand the complexity of the systems which can be manufactured *via* self-assembly by adding another degree of freedom that the designer can manipulate in time as the assembly progresses. This additional degree of freedom can take two forms: either the inter-element affinities can be dynamically switched or the position of the elements themselves can be externally manipulated. The former of these has been demonstrated using switchable hydrophobic/hydrophilic surfaces,^{104,119–121} magnetic forces^{122–124} and thermal/fluid

Table 2 Comparison of stiffness¹ for several trapping devices recently published

Device	Trapped particle, size (nm)	Trapping stiffness (pN nm ⁻¹ W ⁻¹)
Microcavity design (MD)	Polystyrene, 100	3.30
	Polystyrene, 200	7.93
Mode gap design (MG)	Polystyrene, 100	13.1
	Polystyrene, 200	26.85
Microcavity plus hole (MH)	Polystyrene, 100	22.3
Self induced back action ⁷¹	Polystyrene, 100	8.2
	Polystyrene, 50	6.6
Slot waveguides ⁴⁶	Polystyrene, 100	0.2
Plasmonic tweezer ⁶⁸	Polystyrene, 200	0.013
Conventional tweezer ¹⁴	Polystyrene, 500	0.16

conditions.^{121,125–127} While these techniques provide much greater degrees of flexibility, the difficulty in manufacturing assembly elements with sufficient infrastructure that enables one to control the local affinity largely limits the techniques to relatively large elements (typically between 100 μm and 5 mm). Smaller than this, the second option must be used and the assembly guided by direct manipulation of the assembly elements themselves.

On the microscale the most precise method of directing assembly processes is through the use of traditional optical tweezers^{24,128,129} which can manipulate and assemble particles in a way analogous to what we think of as “pick-and-place” assembly on the macroscale. Independent of the specific implementation it is ultimately the precision and parallelity with which the process can be carried out that makes this technique so attractive. Taking advantage of this researchers have recently demonstrated optically driven assembly of 2D¹³⁰ and 3D^{131–133} photonic crystals, nanowires arrays¹³⁴ and a variety of functional fluidic components.¹³⁵

4.2.1 Opportunities for nanophotonic trapping in directed nanoassembly. As described in section 2.2 the useful range of optical tweezers to dielectric targets with sizes larger than about 100 nm.^{24,25} Their applicability to the directed assembly of general nanoscale materials is therefore limited in the same way that they are for the other applications discussed here. As such we will not expand on that further here but will instead focus on the additional challenges directed assembly brings.

(1) *High trap stiffness and positional certainty.* The first additional complication involved in directed assembly is that extremely high positional certainty is required in order to create accurate assemblies. In optical trapping the positional uncertainty is usually described in terms of the trap stiffness or the slope of the force-displacement relationship about the equilibrium point as shown in eqn (5),

$$k\langle x^2 \rangle = k_b T \quad (5)$$

where k is the effective stiffness of the trap and $\langle x^2 \rangle$ is the mean deviation of a trapped particles position along one axis. Since $k_b T$ is fixed for a given temperature, it is obvious from eqn (5) that the greater the trap stiffness, the lower the uncertainty in the position.

Table 2 below compares the normalized trap stiffnesses for some recently demonstrated nanophotonic trapping techniques

in comparison with that for a standard optical tweezer (from Serey *et al.*¹⁹). The resonator designs are the same as those shown in Fig. 10. As can be seen nanophotonic techniques offer as much as two orders of magnitude greater stiffnesses than what can be accomplished with traditional optical tweezers, making them more appropriate for such applications.

(2) *Ability to perform complex handling manoeuvres by exploiting frequency dependence of trapping.* The second additional challenge is that directed nanoassembly, by its nature, requires the ability to actively handle materials rather than just trap (as with single molecule analysis) or transport them (as with optical chromatography). With free space systems, the light field can be sculpted relatively easy to provide this level of positional control. Nanophotonic devices however are hard wired into the substrate and thus arbitrary placement is not possible.

This limitation can be compensated for by exploiting the other handle that the use of optical resonators provide, which is frequency. As discussed in section 3.2 by tuning the wavelength of the excitation light we can essentially turn on and off optically resonant traps. Using evanescently coupled resonators equivalently enables one to turn on and off individual trap sites at different points along a single waveguide. An example of how this can be accomplished is shown in Fig. 11 and uses the same 1D optical resonator structure shown in Fig. 7. Here the waveguide is excited at the resonant wavelength with the guided mode propagating upwards (in the figure). In Fig. 11(a), a 500-nm particle is trapped on the waveguide (yellow circle) and is transported towards the resonator. When the particle arrives in the vicinity of the resonator centre it hops from the waveguide onto the resonator centre and remains trapped on the resonator (orange circles). After evaluation of the particle and the determination of its suitability to join the assembly we de-tune the

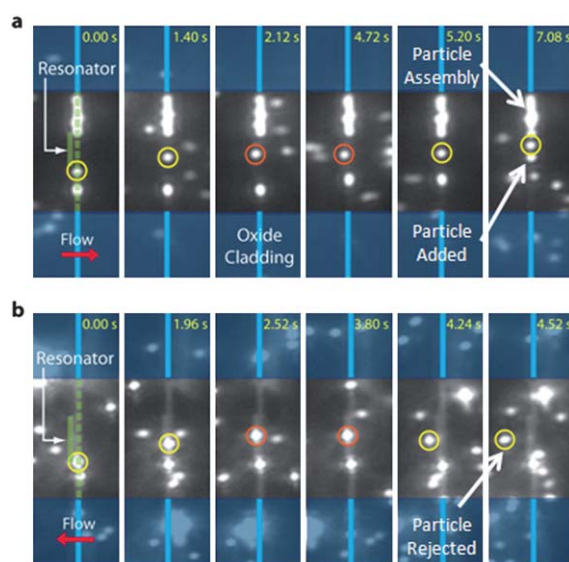


Fig. 11 Directing an assembly using optically resonant particle traps. Experimental demonstration of a controlled nanoparticle assembly using the resonator architecture. (a) Adding a particle to the assembly. (b) Removing one. Further details are provided in the text. Reprinted with permission from Mandal *et al.*⁵⁶ Copyright 2010 American Chemical Society.

wavelength away from resonance and this releases the particle from the resonator back onto the waveguide (since the flow is from left to right) after which it continues to be transported upwards and joins the assembly. In Fig. 11(b) it is shown that simply by reversing the direction of flow in the microfluidic channel the particle can be rejected into the fluidic channel after it is initially transported and trapped at the resonator centre.

4.3 Optical nanofluidics and optical chromatography

The final application area we will discuss here relates to the use of nanophotonic devices for species transport. We separate this subsection into two areas the first discussing the advantages of optical transport in place of traditional nanofluidics and the second discussing the advantages of optically based chromatography.

4.3.1 Opportunities for “optical nanofluidics”. To begin let’s consider the case for the development of an alternative nanoscale transport technique, that I will refer to herein as “optical nanofluidics”. Nanofluidics is often defined as the study of fluid mechanics and transport in systems where the fundamental length scale is less than 100 nm. From a transport point of view, this length scale actually has no actual physical importance and so it perhaps more appropriate to define nanofluidics as fluid flow and transport in channels where electrical double layer overlap becomes significant. We will expand on this a little later, but those unfamiliar with electrokinetics may want to consult one of a number good texts on the subject for more details.^{136–138} Like much of what has been discussed here, the most well developed applications for nanofluidics revolve around sensing, detection, and species handling in single or “few” molecule environments. Put simply, the advantage of using nanofluidics is that it allows for the volume in which the target is confined to be matched to the same spatial scale as that of the target itself.

Unfortunately, the characteristic that makes nanofluidics so interesting is also what limits its practical implementation; size. Because the channels are so small, the speed and volumetric flow rate with which liquids can be transported through them is excruciatingly low. Traditional transport methods such as pressure drop¹³⁹ or electroosmosis^{33,136–138,140} are not effective (see Stone *et al.*¹⁴¹ for an excellent review). The velocity that can be achieved by a pressure drop is proportional to the square of the channel diameter and thus the flow rate become vanishingly small in small channels. Electroosmosis, where flow and transport is induced through the interaction of an applied electric field, has a similar limitation in that velocity scales as $1-1/\kappa d$, where κd is proportional to the channel height. When κd is on the order of 1 (as it is in a nanofluidic systems with double layer overlap) the flow is nearly entirely impeded. Beyond the size limitations these techniques have additional limitations. For example, the parabolic velocity profile associated with pressure driven flow is well known to induce strong sample dispersion¹⁴² which is undesirable in separation applications. In practice electrokinetic techniques are also compatible only with a limited class of fluids (low ionic concentration, aqueous solutions), exhibit extreme sensitivity to surface conditions and generally cannot be used with semiconductor substrates such as silicon.

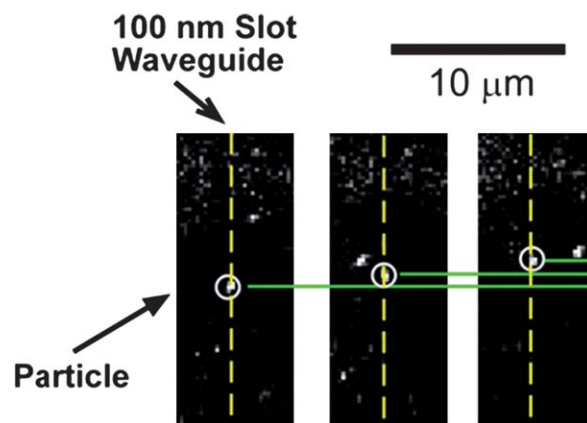


Fig. 12 Transport of dielectric nanomaterials in slot waveguides. Time lapse image of trapped 100 nm nanoparticles in 120 nm slot waveguides are transported a short distance by radiation pressure. Reprinted with permission from Yang *et al.*⁴⁶

In section 3.1 we demonstrated the use of slot waveguides for trapping of DNA. Analogous to what was demonstrated in Fig. 2 for ridge waveguides, because these slots support a propagating mode they can be used to transport small nanoparticles as well. An example of this for 100 nm particles in a 120 nm slot waveguide is shown in Fig. 12. As reported in Yang *et al.*⁴⁶ transport velocities were on the order of $1.5 \mu\text{m s}^{-1}$. Although these experiments are relatively preliminary, there are a couple of reasons why further development of this technique may lead to an advantageous nanofluidic transport technique compared with the state of the art. Many of the advantages discussed above also apply here (in particular the ability to dynamically manipulate the external environment) and there are a few other ones as well.

(1) *Favourable transport scaling laws.* As mentioned above, the optical transport velocity is proportional to the local intensity which itself is inversely proportional to the cross sectional area over which the light is spread (see eqn (3)). As such as the device size gets smaller (in this case the slot waveguide), the transport velocity increases! This is in direct contrast to all other transport methods described above. Using slot waveguide type photonic devices it is possible to shrink the accessible optical energy down to as little as 100 nm by 50 nm. At these scales absolute transport velocities on the order of millimetres per second or greater are achievable.

(2) *Insensitivity to surface/solution conditions.* As mentioned above, electrokinetic techniques are compatible only with a limited class of fluids, exhibit extreme sensitivity to surface conditions and are difficult to use with semiconductor substrates such as silicon (as it relies on an insulating substrates). Nanoscale optofluidic transport is much less dependent on these conditions and can be used in a broader class of systems. This advantage is also similarly apply to many of the other applications listed above.

4.3.2 Opportunities for nanophotonic trapping in optical chromatography. Modern optical chromatography originates from a series of papers by Imasaka and coworkers^{143–146} who

Table 3 Comparison of bioanalytical separation techniques

Technique	Operating principle	Separation velocity
Optical Electrophoresis	Scattering force dependence on particle size and refractive index. $V_{op} \propto I$. Differences in species charge to drag ratio represented by electrophoretic mobility. $V_{ep} \propto E$.	$V_{op} \propto a^5$, $V_{op} \propto (\epsilon_p - \epsilon_m)^2 (\lambda > a)$ $V_{ep} \propto \zeta \neq f(a)^a$ (thin EDL) $V_{ep} \propto 1/a^a$ (thick EDL)
Dielectrophoresis	Lorenz force dependence on particle size and polarizability. $V_{dep} \propto \nabla(E^2)$.	$V_{dep} \propto a^2$ $V_{dep} \propto (\epsilon_p - \epsilon_m)$
Centrifugation	Differences in density. Driving force is gravitational or centrifugal acceleration field, $V_{cent} \propto g$.	$V_{cent} \propto (\rho_p - \rho_m)a^2 \approx a$
Size exclusion chromatography	Size dependence on permeability through packed column. Typically $V_{SEC} \propto \Delta P$	$V_{SEC} \propto -\log(a^3)^b$

^a For free solution electrophoresis. Gel based electrophoresis results in a non-linear drag which can increase the dependence of V_{ep} on a . ^b Approximate, based on assumption of proportionality between hydrodynamic volume and molecular weight.

provided the initial foundations for optically driven separation techniques (see a recent review by Zhao *et al.*¹⁴⁷). The basic idea behind such systems is that when an initially mixed group of particles is subjected to an intense optical field, they can be separated out (fractionated) into different homogeneous groups due to differences in the propulsion velocity based on size or dielectric constant. These works have recently been extended by a number of other researchers including Hart *et al.* who have demonstrated refractive index separation of colloids¹⁴⁸ and other bioparticles.¹⁴⁹ They have also recently integrated this into a microfluidic device format for pathogen detection,¹⁵⁰ demonstrating very precise separation between very closely related bacteria *Bacillus anthracis* and *Bacillus thuringiensis* and millimetre scale separation.¹⁵¹

There are a number of reasons why optical chromatography is of practical interest. As with the other applications, we review two of them here.

(1) Extreme sensitivity of propulsion velocity to particle size.

The most fundamental advantage of using optics for separations comes from the velocity relations shown in Table 3. This table directly compares the fractionalization resolution of various chromatographic techniques with optical methods. As can be seen in the table for the $a < \lambda$ regime the 5th power dependence on the particle size exceeds the nearest competitor (dielectrophoresis) by 3 powers suggesting an optofluidic system should be able to achieve higher resolution.

The most common way to quantify separation resolutions is to compare the spatial separation between two species at some point downstream and divide the difference between the width of the concentration profiles. If we assume that the peak widths will be roughly the same for all systems, it can be shown that the spatial separation divided by the distance travelled, describing the non-dimensional separation resolution, R , is given by

$$R = |l_1(r = a) - l_2(r = a + \Delta a)|/l_1(r = a) \quad (6)$$

where l_1 and l_2 are the distances travelled by particles of radius a and $a + \Delta a$. Using the separation velocities from Table 1 the following relations can be derived for optical, R_{op} , and electrophoretic separations, R_{ep} ,

$$R_{op} = (1 + \Delta a/a)^5 - 1 \quad (7a)$$

$$R_{ep} = 1 - a/(a + \Delta a) \quad (7b)$$

which is valid for the $a \ll \lambda$ case. We compare the separation resolution with electrophoresis, rather than dielectrophoresis for reasons that will be explained in the next paragraph. For $\Delta a/a = 0.01$ (1% size difference) we obtain $R_{op} = 0.051$ and $R_{ep} = 0.0099$ whereas for $\Delta a/a = 0.1$ (10% size difference) yields $R_{op} = 0.61$ and $R_{ep} = 0.09$. This represents a 500% improvement in fractionalization resolution over the state of the art in the small size difference regime and 680% improvement in the large size difference regime.

(2) *Very long interaction length.* Despite this relatively poor comparison in terms of resolution, the reason why techniques such as electrophoresis are successful is not because they fundamentally very size sensitive but rather that the separation impulse can be applied over very long distances. Electrophoresis for example is carried out in capillaries that are 10s of centimetres long. As mentioned in section 2, the use of waveguiding allows us to apply the optical impulse over indefinitely long distances allowing the optical separation impulse to be applied over very long distances as well. Recent works demonstrating the transport of particles in liquid core photonic crystal fibers have shown transport well over cm scale distances.⁴² This combined with the fundamental resolution improvements described above, the achievable optofluidic separation resolution should be at least an order of magnitude greater than the state of the art.

5.0 Summary

In this article we have reviewed near field optical trapping techniques and their applicability to the direct manipulation of nanoscale materials. We have attempted to show there are significant advantages to the use of these techniques for the direct handling of dielectric targets between 5 nm and 100 nm in diameter. In addition to reviewing the state of the art in photonic and plasmonic implementations, we have speculated on a few application areas in which these techniques could have significant technological impact.

Acknowledgements

Elements of this work were funded by: (1) the US National Science Foundation under awards "NIRT: Active

Nanophotofluidic Systems for Single Molecule/Particle Analysis” (Award number 0708599) and “CAREER: Optofluidics - Fusing Microfluidics and Photonics” (Award number 0846489); (2) the US Department of Energy under award “Directed assembly of hybrid nanostructures using optically resonant nanotweezers” (Award number DE-SC0003935); (3) the US National Institutes of Health under award “Optically Resonant Nanotweezers” (Award Number 1R21EB009202-01A2). YFC was partially supported by a post-doctoral fellowship from the Kavli Nanoscience Institute at Cornell. Experimental results presented in this paper were performed in part at the Cornell NanoScale Facility, a member of the National Nanotechnology Infrastructure Network, which is supported by the US National Science Foundation (Grant ECS-0335765).

Notes and references

- 1 D. G. Grier, *Nature*, 2003, **424**, 810–816.
- 2 S. L. Neale, M. P. Macdonald, K. Dholakia and T. F. Krauss, *Nat. Mater.*, 2005, **4**, 530–533.
- 3 M. M. Wang, E. Tu, D. E. Raymond, J. M. Yang, H. C. Zhang, N. Hagen, B. Dees, E. M. Mercer, A. H. Forster, I. Kariv, P. J. Marchand and W. F. Butler, *Nat. Biotechnol.*, 2005, **23**, 83–87.
- 4 J. E. Curtis, B. A. Koss and D. G. Grier, *Opt. Commun.*, 2002, **207**, 169–175.
- 5 M. P. MacDonald, G. C. Spalding and K. Dholakia, *Nature*, 2003, **426**, 421–424.
- 6 P. Y. Chiou, A. T. Ohta and M. C. Wu, *Nature*, 2005, **436**, 370–372.
- 7 M. Krishnan, J. Park and D. Erickson, *Opt. Lett.*, 2009, **34**, 1976–1978.
- 8 L. Novotny, in *Near-Field Optics and Surface Plasmon Polaritons*, ed. S. Kawata, Springer, Amsterdam, 2001.
- 9 B. Saleh and M. Teich, *Fundamentals of Photonics*, John Wiley and Sons, Inc., New York, New York, 1991.
- 10 C. Pollock and M. Lipson, *Integrated Photonics*, Kluwer, Norwell, Massachusetts, 2003.
- 11 K. Svoboda and S. M. Block, *Opt. Lett.*, 1994, **19**, 930–932.
- 12 L. N. Ng, B. J. Luff, M. N. Zervas and J. S. Wilkinson, *J. Lightwave Technol.*, 2000, **18**, 388–400.
- 13 L. N. Ng, M. N. Zervas, J. S. Wilkinson and B. J. Luff, *Appl. Phys. Lett.*, 2000, **76**, 1993–1995.
- 14 K. C. Neuman and S. M. Block, *Rev. Sci. Instrum.*, 2004, **75**, 2787–2809.
- 15 H. Y. Jaising and O. G. Helleso, *Opt. Commun.*, 2005, **246**, 373–383.
- 16 Y. Harada and T. Asakura, *Opt. Commun.*, 1996, **124**, 529–541.
- 17 E. Almaas and I. Brevik, *J. Opt. Soc. Am. B*, 1995, **12**, 2429–2438.
- 18 A. J. H. Yang and D. Erickson, *Nanotechnology*, 2008, **19**, 045704.
- 19 X. Serey, S. Mandal and D. Erickson, *Nanotechnology*, 2010, **21**, 305202.
- 20 K. Dholakia and P. J. Reece, in *Structured Light and Its Applications*, ed. D. L. Andrews, Academic Press, Amsterdam, 2008, pp. 107–138.
- 21 R. Quidant, D. Petrov and G. Badenes, *Opt. Lett.*, 2005, **30**, 1009–1011.
- 22 I. Brevik, T. A. Sivertsen and E. Almaas, *J. Opt. Soc. Am. B*, 2003, **20**, 1739–1749.
- 23 M. Born and E. Wolf, *Principles of Optics*, 6 edn, Pergamon Press Ltd., London, 2003.
- 24 A. Ashkin, J. M. Dziedzic, J. E. Bjorkholm and S. Chu, *Opt. Lett.*, 1986, **11**, 288–290.
- 25 D. T. Chiu and R. N. Zare, *J. Am. Chem. Soc.*, 1996, **118**, 6512–6513.
- 26 A. S. Zelenina, R. Quidant, G. Badenes and M. Nieto-Vesperinas, *Opt. Lett.*, 2006, **31**, 2054–2056.
- 27 P. J. Pauzauskie, A. Radenovic, E. Trepagnier, H. Shroff, P. D. Yang and J. Liphardt, *Nat. Mater.*, 2006, **5**, 97–101.
- 28 S. M. Mansfield, W. R. Studenmund, G. S. Kino and K. Osato, *Opt. Lett.*, 1993, **18**, 305–307.
- 29 J. Guerra, D. Vezenov, P. Sullivan, W. Haimberger and L. Thulin, *Jpn. J. Appl. Phys., Part 1*, 2002, **41**, 1866–1875.
- 30 I. Ichimura, S. Hayashi and G. S. Kino, *Appl. Opt.*, 1997, **36**, 4339–4348.
- 31 G. Baffou, R. Quidant and C. Girard, *Appl. Phys. Lett.*, 2009, **94**.
- 32 G. Baffou, C. Girard and R. Quidant, *Phys. Rev. Lett.*, 2010, **104**.
- 33 D. Erickson, D. Sinton and D. Q. Li, *Lab Chip*, 2003, **3**, 141–149.
- 34 S. Kawata and T. Sugiura, *Opt. Lett.*, 1992, **17**, 772–774.
- 35 S. Kawata and T. Tani, *Opt. Lett.*, 1996, **21**, 1768–1770.
- 36 L. N. Ng, B. J. Luff, M. N. Zervas and J. S. Wilkinson, *Opt. Commun.*, 2002, **208**, 117–124.
- 37 K. Grujic, O. G. Helleso, J. P. Hole and J. S. Wilkinson, *Opt. Express*, 2005, **13**, 1–7.
- 38 S. Gaugiran, S. Getin, J. M. Fedeli, G. Colas, A. Fuchs, F. Chatelain and J. Derouard, *Opt. Express*, 2005, **13**, 6956–6963.
- 39 T. Tanaka and S. Yamamoto, *Appl. Phys. Lett.*, 2000, **77**, 3131–3133.
- 40 K. Grujic and O. G. Helleso, *Opt. Express*, 2007, **15**, 6470–6477.
- 41 B. S. Schmidt, A. H. J. Yang, D. Erickson and M. Lipson, *Opt. Express*, 2007, **15**, 14322–14334.
- 42 S. Mandal and D. Erickson, *Appl. Phys. Lett.*, 2007, **90**, 184103.
- 43 H. Schmidt and A. R. Hawkins, *Microfluid. Nanofluid.*, 2008, **4**, 3–16.
- 44 A. R. Hawkins and H. Schmidt, *Microfluid. Nanofluid.*, 2008, **4**, 17–32.
- 45 S. Kuhn, B. S. Phillips, E. J. Lunt, A. R. Hawkins and H. Schmidt, *Lab Chip*, 2010, **10**, 189–194.
- 46 A. H. J. Yang, S. D. Moore, B. S. Schmidt, M. Klug, M. Lipson and D. Erickson, *Nature*, 2009, **457**, 71–75.
- 47 A. H. J. Yang, T. Lerdsuchatawanich and D. Erickson, *Nano Lett.*, 2009, **9**, 1182–1188.
- 48 C. A. Barrios and M. Lipson, *Opt. Express*, 2005, **13**, 10092–10101.
- 49 S. Lin, E. Schonbrun and K. Crozier, *Nano Lett.*, 2010, **10**, 2408–2411.
- 50 F. Vollmer and S. Arnold, *Nat. Methods*, 2008, **5**, 591–596.
- 51 C. R. Pollock and M. Lipson, *Integrated photonics*, Kluwer Academic, Boston; London, 2003.
- 52 A. H. J. Yang and D. Erickson, *Lab Chip*, 2010, **10**, 769–774.
- 53 S. Arnold, D. Keng, S. I. Shopova, S. Holler, W. Zurawsky and F. Vollmer, *Opt. Express*, 2009, **17**, 6230–6238.
- 54 J. D. Joannopoulos, R. D. Meade and J. W. Winn, *Photonic Crystals: Molding the Flow of Light*, Princeton University Press, Princeton, New Jersey, 1995.
- 55 J. S. Foresi, P. R. Villeneuve, J. Ferrera, E. R. Thoen, G. Steinmeyer, S. Fan, J. D. Joannopoulos, L. C. Kimerling, H. I. Smith and E. P. Ippen, *Nature*, 1997, **390**, 143–145.
- 56 S. Mandal, X. Serey and D. Erickson, *Nano Lett.*, 2010, **10**, 99–104.
- 57 G. Mie, *Ann. Phys.*, 1908, **25**, 377–445.
- 58 R. H. Ritchie, *Phys. Rev.*, 1957, **106**, 874–881.
- 59 J. A. Schuller, E. S. Barnard, W. S. Cai, Y. C. Jun, J. S. White and M. L. Brongersma, *Nature Materials*, 9, pp. 193–204.
- 60 J. Henzie, J. Lee, M. H. Lee, W. Hasan and T. W. Odom, *Annu. Rev. Phys. Chem.*, 2009, **60**, 147–165.
- 61 J. Homola, *Chem. Rev.*, 2008, **108**, 462–493.
- 62 S. A. Maier and H. A. Atwater, *J. Appl. Phys.*, 2005, **98**, 011101.
- 63 R. Quidant and C. Girard, *Laser Photonics Rev.*, 2008, **2**, 47–57.
- 64 G. Volpe, R. Quidant, G. Badenes and D. Petrov, *Phys. Rev. Lett.*, 2006, **96**.
- 65 T. Cizmar, M. Siler, M. Sery, P. Zemanek, V. Garces-Chavez and K. Dholakia, *Phys. Rev. B*, 2006, **74**.
- 66 M. Righini, A. S. Zelenina, C. Girard and R. Quidant, *Nat. Phys.*, 2007, **3**, 477–480.
- 67 M. Righini, G. Volpe, C. Girard, D. Petrov and R. Quidant, *Phys. Rev. Lett.*, 2008, **100**.
- 68 A. N. Grigorenko, N. W. Roberts, M. R. Dickinson and Y. Zhang, *Nat. Photonics*, 2008, **2**, 365–370.
- 69 L. Huang, S. J. Maerkl and O. J. F. Martin, *Opt. Express*, 2009, **17**, 6018–6024.
- 70 W. H. Zhang, L. N. Huang, C. Santschi and O. J. F. Martin, *Nano Lett.*, 2010, **10**, 1006–1011.
- 71 M. L. Juan, R. Gordon, Y. J. Pang, F. Eftekhari and R. Quidant, *Nat. Phys.*, 2009, **5**, 915–919.
- 72 K. Wang, E. Schonbrun and K. B. Crozier, *Nano Lett.*, 2009, **9**, 2623–2629.
- 73 K. Wang, E. Schonbrun, P. Steinvurzel and K. B. Crozier, *Nano Lett.*, 2010, **10**, 3506–3511.
- 74 A. Borgia, P. M. Williams and J. Clarke, *Annu. Rev. Biochem.*, 2008, **77**, 101–125.

- 75 W. E. Moerner, *Proc. Natl. Acad. Sci. U. S. A.*, 2007, **104**, 12596–12602.
- 76 B. Schuler and W. A. Eaton, *Curr. Opin. Struct. Biol.*, 2008, **18**, 16–26.
- 77 V. N. Uversky, A. V. Kabanov and Y. L. Lyubchenko, *J. Proteome Res.*, 2006, **5**, 2505–2522.
- 78 J. Groll, E. V. Amirgoulouva, T. Ameringer, C. D. Heyes, C. Rocker, G. U. Nienhaus and M. Moller, *J. Am. Chem. Soc.*, 2004, **126**, 4234–4239.
- 79 Y. W. Jia, D. S. Talaga, W. L. Lau, H. S. M. Lu, W. F. DeGrado and R. M. Hochstrasser, *Chem. Phys.*, 1999, **247**, 69–83.
- 80 X. H. N. Xu and E. S. Yeung, *Science*, 1998, **281**, 1650–1653.
- 81 E. Mei, J. Y. Tang, J. M. Vanderkooi and R. M. Hochstrasser, *J. Am. Chem. Soc.*, 2003, **125**, 2730–2735.
- 82 E. Rhoades, E. Gussakovskiy and G. Haran, *Proc. Natl. Acad. Sci. U. S. A.*, 2003, **100**, 3197–3202.
- 83 B. Okumus, T. J. Wilson, D. M. J. Lilley and T. Ha, *Biophys. J.*, 2004, **87**, 2798–2806.
- 84 J. O. Tegenfeldt, C. Prinz, H. Cao, S. Chou, W. W. Reisner, R. Riehn, Y. M. Wang, E. C. Cox, J. C. Sturm, P. Silberzan and R. H. Austin, *Proc. Natl. Acad. Sci. U. S. A.*, 2004, **101**, 10979–10983.
- 85 D. Huh, K. L. Mills, X. Y. Zhu, M. A. Burns, M. D. Thouless and S. Takayama, *Nat. Mater.*, 2007, **6**, 424–428.
- 86 P. Sivanesan, K. Okamoto, D. English, C. S. Lee and D. L. DeVoe, *Anal. Chem.*, 2005, **77**, 2252–2258.
- 87 W. E. Moerner, *J. Phys. Chem. B*, 2002, **106**, 910–927.
- 88 I. Braslavsky, E. Kartalov, B. Hebert and S. R. Quake, *Biophys. J.*, 2002, **82**, 507A–507A.
- 89 I. Braslavsky, B. Hebert, E. Kartalov and S. R. Quake, *Proc. Natl. Acad. Sci. U. S. A.*, 2003, **100**, 3960–3964.
- 90 A. T. Woolley, C. Guillemette, C. L. Cheung, D. E. Housman and C. M. Lieber, *Nat. Biotechnol.*, 2000, **18**, 760–763.
- 91 A. E. Cohen and W. E. Moerner, *Proc. Natl. Acad. Sci. U. S. A.*, 2006, **103**, 4362–4365.
- 92 A. E. Cohen and W. E. Moerner, *Opt. Express*, 2008, **16**, 6941–6956.
- 93 B. A. Grzybowski, C. E. Wilmer, J. Kim, K. P. Browne and K. J. M. Bishop, *Soft Matter*, 2009, **5**, 1110–1128.
- 94 G. M. Whitesides, J. P. Mathias and C. T. Seto, *Science*, 1991, **254**, 1312–1319.
- 95 S. C. Glotzer, M. J. Solomon and N. A. Kotov, *AIChE J.*, 2004, **50**, 2978–2985.
- 96 E. Winfree, F. R. Liu, L. A. Wenzler and N. C. Seeman, *Nature*, 1998, **394**, 539–544.
- 97 C. A. Mirkin, R. L. Letsinger, R. C. Mucic and J. J. Storhoff, *Nature*, 1996, **382**, 607–609.
- 98 K. Keren, R. S. Berman, E. Buchstab, U. Sivan and E. Braun, *Science*, 2003, **302**, 1380–1382.
- 99 T. H. LaBean, H. Yan, J. Kopatsch, F. R. Liu, E. Winfree, J. H. Reif and N. C. Seeman, *J. Am. Chem. Soc.*, 2000, **122**, 1848–1860.
- 100 H. L. Chen, R. Schulman, A. Goel and E. Winfree, *Nano Lett.*, 2007, **7**, 2913–2919.
- 101 H. Yan, S. H. Park, G. Finkelstein, J. H. Reif and T. H. LaBean, *Science*, 2003, **301**, 1882–1884.
- 102 H. J. J. Yeh and J. S. Smith, *IEEE Photonics Technol. Lett.*, 1994, **6**, 706–708.
- 103 U. Srinivasan, M. A. Helmbrecht, C. Rembe, R. S. Muller and R. T. Howe, *IEEE J. Sel. Top. Quantum Electron.*, 2002, **8**, 4–11.
- 104 X. R. Xiong, Y. Hanein, J. D. Fang, Y. B. Wang, W. H. Wang, D. T. Schwartz and K. F. Bohringer, *J. Microelectromech. Syst.*, 2003, **12**, 117–127.
- 105 W. Zheng, J. Chung and H. O. Jacobs, *J. Microelectromech. Syst.*, 2006, **15**, 864–870.
- 106 A. Avital and E. Zussman, *IEEE Trans. Adv. Packag.*, 2006, **29**, 719–724.
- 107 A. Debray, Y. A. Chapuis, M. Shibata and H. Fujita, *IEICE Electronics Express*, 2006, **3**, 227–232.
- 108 A. M. Kalsin, M. Fialkowski, M. Paszewski, S. K. Smoukov, K. J. M. Bishop and B. A. Grzybowski, *Science*, 2006, **312**, 420–424.
- 109 E. V. Shevchenko, D. V. Talapin, N. A. Kotov, S. O'Brien and C. B. Murray, *Nature*, 2006, **439**, 55–59.
- 110 K. Mitamura, T. Imae, N. Saito and O. Takai, *J. Phys. Chem. B*, 2007, **111**, 8891–8898.
- 111 N. Bowden, F. Arias, T. Deng and G. M. Whitesides, *Langmuir*, 2001, **17**, 1757–1765.
- 112 F. Li, X. Badel, J. Linnros, G. Wasserman, S. L. Whittenburg, L. Spinu and J. B. Wiley, *Adv. Mater.*, 2006, **18**, 270.
- 113 B. A. Grzybowski, M. Radkowski, C. J. Campbell, J. N. Lee and G. M. Whitesides, *Appl. Phys. Lett.*, 2004, **84**, 1798–1800.
- 114 X. Checoury, S. Enoch, C. Lopez and A. Blanco, *Appl. Phys. Lett.*, 2007, 90.
- 115 J. G. Fleming, S. Y. Lin, I. El-Kady, R. Biswas and K. M. Ho, *Nature*, 2002, **417**, 52–55.
- 116 K. H. Lin, J. C. Crocker, V. Prasad, A. Schofield, D. A. Weitz, T. C. Lubensky and A. G. Yodh, *Phys. Rev. Lett.*, 2000, **85**, 1770–1773.
- 117 Y. G. Li, Y. D. Tseng, S. Y. Kwon, L. D'Espaux, J. S. Bunch, P. L. McEuen and D. Luo, *Nat. Mater.*, 2004, **3**, 38–42.
- 118 R. J. Jackman, S. T. Brittain, A. Adams, M. G. Prentiss and G. M. Whitesides, *Science*, 1998, **280**, 2089–2091.
- 119 K. F. Bohringer, *J. Micromech. Microeng.*, 2003, **13**, S1–S10.
- 120 J. Lahann, S. Mitragotri, T. N. Tran, H. Kaido, J. Sundaram, I. S. Choi, S. Hoffer, G. A. Somorjai and R. Langer, *Science*, 2003, **299**, 371–374.
- 121 R. Sharma, *Langmuir*, 2007, **23**, 6843–6849.
- 122 P. White, K. Kopanski and H. Lipson, *IEEE International Conference on Robotics and Automation (ICRA04)*, 2004.
- 123 P. White, V. Zykov and H. Lipson, *Robotics Science and Systems*, 2005.
- 124 S. Griffith, D. Goldwater and J. M. Jacobson, *Nature*, 2005, **437**, 636–636.
- 125 M. T. Tolley, M. Krishnan, D. Erickson and H. Lipson, *Appl. Phys. Lett.*, 2008, 93.
- 126 M. Krishnan, M. T. Tolley, H. Lipson and D. Erickson, *Phys. Fluids*, 2008, 20.
- 127 M. Krishnan, M. T. Tolley, H. Lipson and D. Erickson, *Langmuir*, 2009, **25**, 3769–3774.
- 128 A. Ashkin, *Phys. Rev. Lett.*, 1970, **24**, 156–159.
- 129 A. Ashkin and J. M. Dziedzic, *Appl. Phys. Lett.*, 1971, **19**, 283.
- 130 D. Erenso, A. Shulman, J. Curtis and S. Elrod, *J. Mod. Opt.*, 2007, **54**, 1529–1536.
- 131 D. C. Benito, D. M. Carberry, S. H. Simpson, G. M. Gibson, M. J. Padgett, J. G. Rarity, M. J. Miles and S. Hanna, *Opt. Express*, 2008, **16**, 13005–13015.
- 132 G. Sinclair, P. Jordan, J. Courtial, M. Padgett, J. Cooper and Z. J. Laczik, *Opt. Express*, 2004, **12**, 5475–5480.
- 133 P. Jordan, H. Clare, L. Flendrig, J. Leach, J. Cooper and M. Padgett, *J. Mod. Opt.*, 2004, **51**, 627–632.
- 134 R. Agarwal, K. Ladavac, Y. Roichman, G. H. Yu, C. M. Lieber and D. G. Grier, *Opt. Express*, 2005, **13**, 8906–8912.
- 135 A. Terray, J. Oakey and D. W. M. Marr, *Science*, 2002, **296**, 1841–1844.
- 136 J. Lyklema, *Fundamentals of Interface and Colloid Science, Volume 1: Fundamentals*, Academic Press, London, 1991.
- 137 J. Lyklema, *Fundamentals of Interface and Colloid Science, Volume 2: Solid Liquid Interfaces*, Academic Press, London, 1995.
- 138 D. Li, *Electrokinetics in Microfluidics* Elsevier Academic Boston, 2004.
- 139 M. A. Unger, H. P. Chou, T. Thorsen, A. Scherer and S. R. Quake, *Science*, 2000, **288**, 113–116.
- 140 R. J. Hunter, *Zeta potential in colloid science: principles and applications*, Academic Press, London, 1981.
- 141 H. A. Stone, A. D. Stroock and A. Ajdari, *Annu. Rev. Fluid Mech.*, 2004, **36**, 381–411.
- 142 S. Ghosal, *Annu. Rev. Fluid Mech.*, 2006, **38**, 309–338.
- 143 T. Hatano, T. Kaneta and T. Imasaka, *Anal. Chem.*, 1997, **69**, 2711–2715.
- 144 T. Imasaka, *Analisis*, 1998, **26**, M53–M55.
- 145 J. Makihara, T. Kaneta and T. Imasaka, *Talanta*, 1999, **48**, 551–557.
- 146 T. Kaneta, Y. Ishidzu, N. Mishima and T. Imasaka, *Anal. Chem.*, 1997, **69**, 2701–2710.
- 147 B. S. Zhao, Y. M. Koo and D. S. Chung, *Anal. Chim. Acta*, 2006, **556**, 97–103.
- 148 S. J. Hart and A. V. Terray, *Appl. Phys. Lett.*, 2003, **83**, 5316–5318.
- 149 S. J. Hart, A. Terray, K. L. Kuhn, J. Arnold and T. A. Leski, *American Laboratory*, 2004, **36**, 13.
- 150 A. Terray, J. Arnold and S. J. Hart, *Opt. Express*, 2005, **13**, 10406–10415.
- 151 S. J. Hart, A. Terray, T. A. Leski, J. Arnold and R. Stroud, *Anal. Chem.*, 2006, **78**, 3221–3225.